EKSPLOATACJA I NIEZAWODNOŚĆ MAINTENANCE AND RELIABILITY

# Eksploatacja i Niezawodnosc – Maintenance and Reliability

**Volume 24 (2022), Issue 2**

journal homepage: http://www.ein.org.pl

Article citation info:
Wos S, Koszela W, Dzierwa A, Reizer R, Pawlus P. Effects of oil pocket shape and density on friction in reciprocating sliding. Eksploatacja i Niezawodnosc – Maintenance and Reliability 2022; 24 (2): 338–345, http://doi.org/10.17531/ein.2022.2.15.

# Effects of oil pocket shape and density on friction in reciprocating sliding

Indexed by: Web of Science Group

Slawomir Wos[a], Waldemar Koszela[a], Andrzej Dzierwa[a,*], Rafal Reizer[b], Pawel Pawlus[a]

[a] Rzeszow University of Technology, Department of Manufacturing Technology and Production Engineering, Powstancow Warszawy 8, 35-959 Rzeszow, Poland
[b] University of Rzeszow, Institute of Materials Engineering, College of Natural Sciences, Pigonia 1, 35-310 Rzeszow, Poland

## Highlights

- Laser texturing in most cases led to reductions in friction force values and variations.
- The best tribological behavior was achieved for the pit-area ratio of 9%.
- High friction was obtained for circular dimples of 22% and for sandglass shape dimples of 5% density.
- Surface texturing caused the shift of the maximum friction from the transversal point.

## Abstract

The purpose of this work is to study the effect of oil pocket shape and density on friction in reciprocating sliding. The experiments were conducted in reciprocating motion under starved lubrication conditions. Tribological tests were performed using an Optimol SRV5 tribotester. The frictional pair consisted of two discs of 42CrMo4 steel. One disc was laser textured. The oil pockets had circular and sandglass shapes. Disc samples of various texture shapes were characterized by the same pit-area ratios. The operating parameters were the same for all friction pairs. In most cases, surface texturing led to reductions in friction force value and scatter. For both dimple shapes, the best tribological properties were achieved for oil pocket density of 9%. When discs with circular dimples were tested, the highest resistance to motion was received for the highest pit-area ratio of 9%. On the contrary, the worst tribological performance of discs with sandglass-shaped oil pockets of sandglass shape were obtained for the largest oil pocket density of 22%.

## Keywords

laser texturing, reciprocating motion, friction.



## 1. Introduction

Frictional forces may be beneficial, but they also oppose to motion. In some cases friction should be high [14, 25]. On the other hand, friction between machine elements reduces the efficiency of the machine. For example, in passenger cars, one-third of the fuel energy is applied to overcome friction [10]. Therefore the efforts of minimizing friction are of substantial importance. Modification of surface topography of sliding element is one of methods of friction reduction. Surface texturing is an option for an improvement in functional performance of machine elements by creating dimples (oil pockets or cavities) or valleys on sliding surfaces. It leads to a reduction in friction, usually in mixed and boundary lubrications. Surface texturing also caused an increase in seizure resistance. Dimples can also be traps to wear debris, improving resistance to abrasion. Many works have been devoted to surface texturing, including reviews [2, 4, 5, 20, 23]. Gachot et al. [5] presented positive and negative tribological effects of surface texturing. Rosenkranz et al. [23] analysed the applications of surface texturing with a special attention to piston rings, seals, gears and roller bearings. Etsion [4] reviewed efforts in the field of laser surface texturing. Nilsson et al. [20] took into consideration mechanisms of friction reduction due to surface texturing. Atulkar et al. [2] analysed the advantages of piston rings and cylinder liners texturing. Typically, the experiments in this topic were conducted in unidirectional sliding. The results of tests in reciprocating motions are more difficult to interpret because in various places of sliding parts different conditions occur.

The plateau honing of the cylinder liners is one of the first examples of surface texturing. The surface after plateau honing of the cross-hatched pattern has traces of two honing operations: finish honing and plateau honing. This surface resembles that obtained after running-in. It is characterized by a higher oil capacity than the cylinder liner after the one-process honing, resulting in higher oil consumption and a smaller tendency to scuffing. The wear of the two-process cylinder surface is smaller than that of the one-process surface characterized by a similar roughness height after engine test [21] and laboratory simulation [8]. Two-process cylinder surfaces led also to the improvement of engine performance such as an increase in power and a decrease in fuel consumption [24] and a reduction in friction torque [32], as well as a decrease in friction reduction in mixed lubrication [9] compared to the behavior of one-process cylinder.

Honing process was also combined with additional texturing. Grabon et al. [7] achieved friction reduction in reciprocating test by

(*) Corresponding author.
E-mail addresses:
S. Wos (ORCID: 0000-0003-4870-1693): wosslawomir@prz.edu.pl , W. Koszela (ORCID: 0000-0002-3476-3992): wkktmiop@prz.edu.pl, A. Dzierwa (ORCID: 0000-0003-4545-1748): adzierwa@prz.edu.pl, R. Reizer (ORCID: 0000-0002-7642-1499): rreizer@ur.edu.pl, P. Pawlus (ORCID: 0000-0002-5630-5300): ppawlus@prz.edu.pl

creating dimples by burnishing technique. Koszela et al. [13] used this technique and obtained an increase in the power of a high performance internal combustion engine. Hua et al. [11] and Kang et al. [12] studied the effects of discriminating partition on Diesel cylinder bore on engine operating parameters. They achieved reductions in fuel and oil consumptions compared to the behavior of the engine with plateau-honed cylinder liners. Yin et al. found that the array of dimples affected the engine torque [31]. In works [11, 12, 31], dimples were created by laser texturing.

The oil pockets used in the works [7, 11, 12, 13, 31] had a circular shape. This shape is commonly applied because of the belief that the effect of shape on the tribological performance of sliding elements is negligible and the machining of circular oil pockets is the cheapest. However, it was found that the shape of the oil pocket shape affected the tribological performance of sliding elements and some techniques allow us to create oil pockets of different shapes at reasonable cost.

The selection of the dimple shape depends on the operating conditions. In unidirectional sliding, the orientation of dimples to sliding direction is important. Zhang et al. [35] after simulation and Wang et al. [29] after experiment found that one side border of triangular dimples should first enter the contact zone. Galda et al. [6] obtained the same finding with regard to drop-shaped oil pockets. The orientation of the chevrons to the sliding direction is also substantial. Wos et al. [30] achieved the best frictional performance for chevrons inclined to the outer sides of the rotating discs. Shen and Khonsari [26] found after simulation that optimum textures for unidirectional sliding have chevrons with flat fronts.

Zhang et al. [36] achieved better tribological behavior of square oil pockets compared to triangular, rectangular, and circular in the reciprocating regime. In [1], reductions in friction and running-in duration were found due to coating and surface texture in reciprocation sliding - the dimples had a trapezoidal shape. This shape was found to be the best for bidirectional sliding under theoretical consideration [26]. Costa and Hutchings [3] found that chevrons produced the highest film thickness compared to grooves and circular dimples in hydrodynamic lubrication under reciprocating motion in line contact regime. Morris et al. [18] obtained a reduction in friction in lubricated reciprocating sliding for low velocity by creating chevrons on sliding surfaces. The highest reduction compared to untextured cylinder liner was achieved for shallow chevrons [19]. Lu et al. [16] achieved a reduction in friction in line contact during reciprocating lubricating sliding due to the presence of square dimples on the flat surface. However, the maximum reduction was not high (15% in boundary lubrication). They analyzed the tribological effects of triangular [15] and square [17] dimples and found that converging dimples led to beneficial behavior. Vladescu et al. [27, 28] and Yuan et al. [34] achieved the superiority of grooves oriented perpendicularly to the sliding direction in lubricated reciprocating motion over their different positions. When film thickness was small, large reductions in friction under the boundary lubrication regime were achieved, the texture with grooves perpendicular to the sliding direction behaved the best [28]. Load support by transverse oil pockets was caused by the occurrence of inlet suction [27]. Grooves perpendicular to the sliding direction led to higher friction reduction under a relatively low contact pressure compared to grooves of parallel orientation [34]. Yu et al. [33] found that elliptical dimples positioned orthogonally to the sliding direction had a higher friction reduction than square and triangular oil pockets.

In this work, the effect of oil pocket shape and density on friction in reciprocating sliding will be experimentally studied. The oil pockets have circular and sandglass shapes. The effect of sandglass-shaped dimples on the tribological performance of sliding elements in bidirectional sliding was not previously studied. This shape resulted from the beneficial effect of triangular oil pockets in unidirectional sliding.

## 2. Experimental details

The experiments were carried out in a starved lubricated reciprocating conformal contact of two steel discs using an Optimol SRV5 tribotester. Both discs were made from 42CrMo4 steel of 44 ± 2 HRC hardness. Before each test, 1 drop of L-AN-46 oil (approximately 0.04 ml) was supplied to the inlet side of the contact zone. The lubricant was not added during each test. The test parameters were the same for all friction pairs: the normal load was 50 N, the oscillation frequency was 20 Hz, and the stroke was 3 mm. The nominal contact pressure was 0.6 MPa. The duration of each test was set to 12500 cycles. The tests were carried out at a temperature of 30°± 0.2°C. Dimples were created on larger discs. Discs were prepared by laser texturing using grinding and lapping. Such treatment was necessary to prevent shape errors of dimples occurring during laser texturing. Test parameters were selected to correspond to working parameters of piston ring – cylinder bore assembly during combustion engine start up. Where frequency of oscillations is small, low temperature occurs and all parts are not fully lubricated. Such conditions do not help to obtain full film lubrication, in this case surface texturing can help to create hydrodynamic film.

Texturing parameters for laser engraver SpeedMarker 300, produced by Trotec® and equipped with a 20 W power ytterbium pulsed fiber laser, were set to obtain dimples of 10-40 µm depth. The parameters of laser texturing are listed in Table 1.

*Table 1. Parameters of laser texturing*

| | | | |
|---|---|---|---|
| **Laser power and type:** | 20 W ytterbium pulsed fiber laser | **Pulse energy:** | near 1 mJ |
| **Pulse duration:** | 1.5 ns | **Repetition rate:** | 1000 kHz |
| **Focal diameter:** | ~45 µm | **Beam driven pattern:** | crosshatch pattern |
| **Spacing between beam passes:** | 0.01 mm | **Marking speed:** | 200 mm/s |

The contact surfaces of the samples and counter-samples were lapped to achieve a roughness parameter Ra of 0.14±0.02 µm before laser texturing. Different dimples were created, with circular and sandglass shapes, and pit-area ratios of 5, 9, 14, 17, and 22% for both shapes. Circular dimples are the most popular. The sandglass shape was the original idea of the authors of this paper. Figure 1 presents photos of all textured discs and the counter sample.

The sliding pair with the untextured disc sample was also tested. The number of test repetitions for the same sliding pair was seven. The friction configuration scheme is presented in Figure 2. The surface textures of the discs were measured before and after the tribological tests using a stylus profilometer Hommel Etamic T8000 with a tip radius of 2 µm. Measured surfaces were only leveled, and digital filtration was not used.

Worn surfaces were also analyzed using Phenom ProX desktop SEM microscopy.

## 3. Results and discussion

Figure 3 and Figure 4 present the contour plots and extracted profiles of the selected textured disc surfaces.

The densities of the oil pockets resulted from their sizes. The depths of dimples of the circular shape were typically between 12 and 15 µm, except for the smallest density of 5% - in this case, the depths of the dimples were near 35 µm and the density of 9% for which the depths were about 20 µm. The bottoms of the circular dimples were sym-

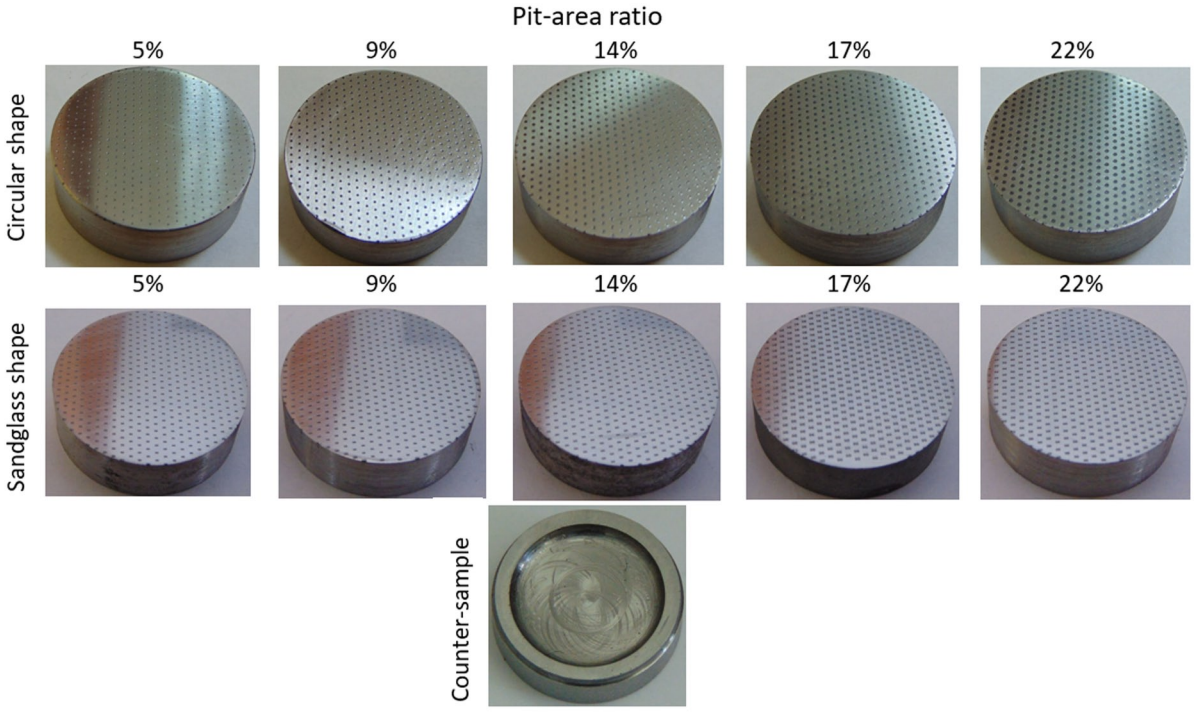


*Fig. 1. Photos of textured disc surfaces and of counter sample before the tests*

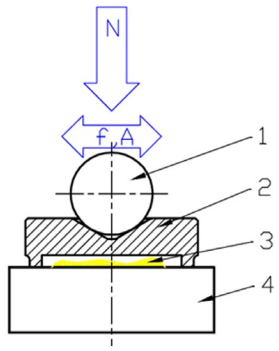


*Fig. 2. Schematic of friction configuration; N – normal load, f - frequency, A - amplitude; 1 - ball which transfers load and movement to the counter sample, 2- self-aligning counter sample, 3 - supplied oil, 4- stationary disc textured or untextured sample*

metrical. For three largest oil pockets (densities of 14, 17 and 22%), the bottoms had shapes similar to W letter.

The depths of the oil pockets of sandglass shape were typically between 30 and 40 µm, only the depths of the largest dimples (a density of 22%) were smaller, near 20 µm. The bottoms of most oil pockets had shapes similar to W letter, only the oil pockets of the middle pit-area ratio (14%) were the exceptions. The largest dimples with densities of 17 and 22% had a non-symmetrical shape in contrast to other oil pockets.

Figures 5, 6 present the courses of the coefficient of friction of sliding pairs with textured oil pockets.

One can see from the analysis of Figure 5 and Figure 6 that the resistance to motion of the textured assemblies after the initial fluctuations decreased as the tests progressed. When the disc with spherical dimples of the smallest pit-area ratio was tested, the coefficient of friction decreased from the range: 0.05-0.1 to the range: 0.03-0.06. The increase in dimple density to 9% caused smaller scatters of the coefficient of friction, which decreased from: 0.04-0.07 to 0.03-0.04. A further increase in the pit-area ratio to 14% caused an increase in the coefficient of friction; it decreased from 0.09-0.11 to 0.04-0.06. When the dimple density was 17%, the scatter of the coefficient of friction was large: the friction coefficient decreased

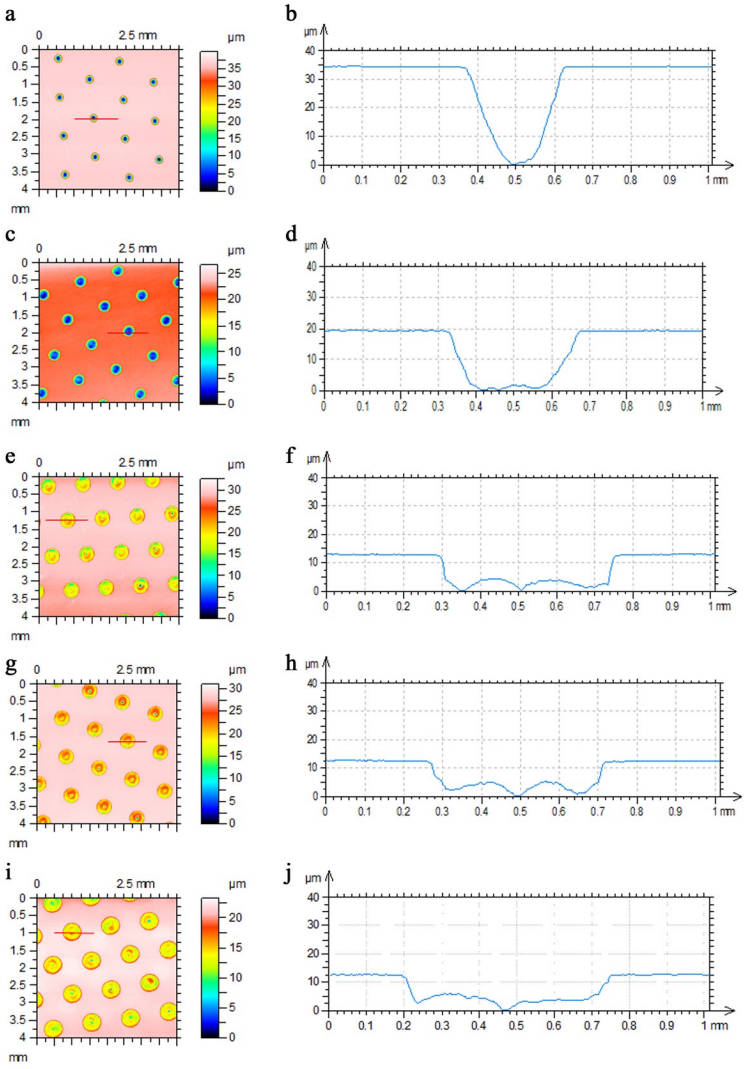


*Fig. 3. Contour plots (a, c, e, g, i) and extracted profiles of circular-shaped textured disc samples of circular shape with pit-area ratio of 5 (a, b), 9 (c, d), 14 (e, f) 17 (g, h) and 22% (i, j)*

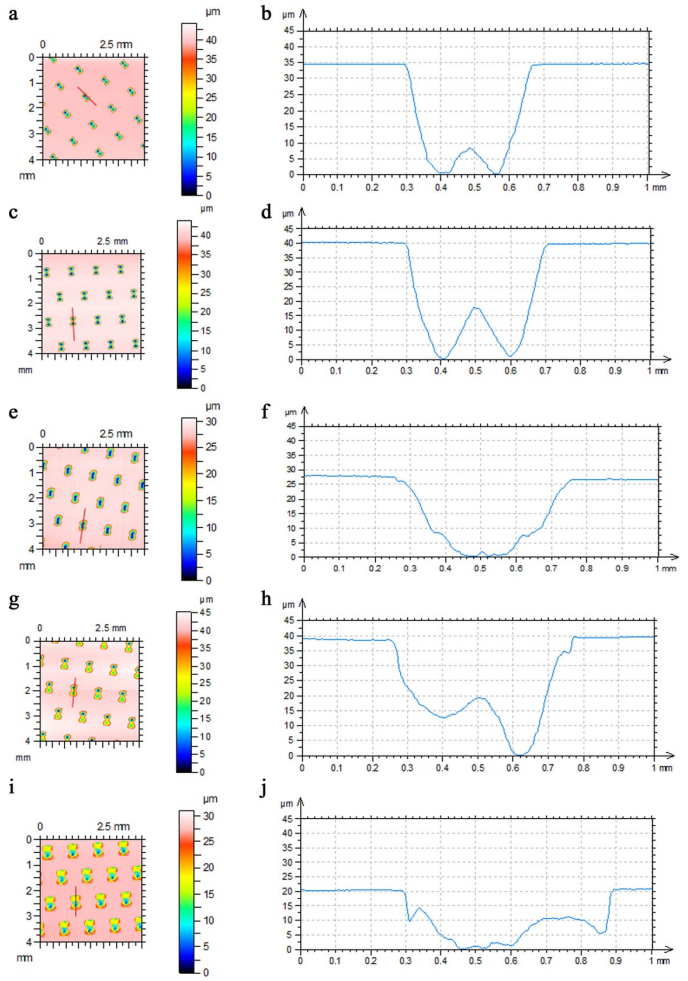


*Fig. 4. Contour plots (a, c, e, g, i) and extracted profiles of textured disc samples of sandglass shape with pit-area ratio of 5 (a, b), 9 (c, d), 14 (e, f) 17 (g,h) and 22% (i, j)*

from the range: 0.080.13 to the range: 0.03-0.08. The highest pit-area ratio of 22% caused increases in resistance to motion and in scatter of the final friction coefficient; the coefficient of friction decreased from 0.25-0.27 to 0.06-0.14.

The smallest scatters and coefficients of friction were achieved for the textured disc sample of sandglass shape with the pit-area ratio of 9%. The coefficient of friction decreased from the range: 0.055-0.7 to 0.03-0.035. A further increase in oil pocket density led to increases in the coefficient of friction and its scatter. When the pit-area ratio was 14%, the coefficient of friction decreased from 0.06-0.15 to 0.03-0.08. Those scatters were a little smaller for dimple density of 17% and amounted to 0.07-0.09 in the initial parts of the tests and 0.04-0.055 finally. When the pit-area ratio of the disc sample was the highest of 22%, the coefficient of friction decreased from 0.1-0.16 to 0.04-0.05. However, among sliding pairs with textured discs of sandglass shape, the highest average values and scatters of the coefficient of friction were obtained for the smallest oil pocket density of 5%; during tests, the coefficient of friction decreased from 0.12-0.26 to 0.04-0.15.

Figure 7 presents the runs of the coefficient of friction for the untextured sliding assembly. In most cases, the courses of the coefficient of friction were different from those obtained for textured assemblies. After the initial fluctuation, the coefficient of friction slowly increased. It reached maximum value after about 500 seconds and then gradually decreased. The coefficient of friction after 500 seconds was in the range: 0.045-0.275, but in the final part of tests in the range: 0.035-0.27. In this case, both average value and scatter of the friction coefficient were high.

It is evident from the analysis of Table 2 that the final coefficient of friction was smaller than the initial coefficient of friction. This behavior

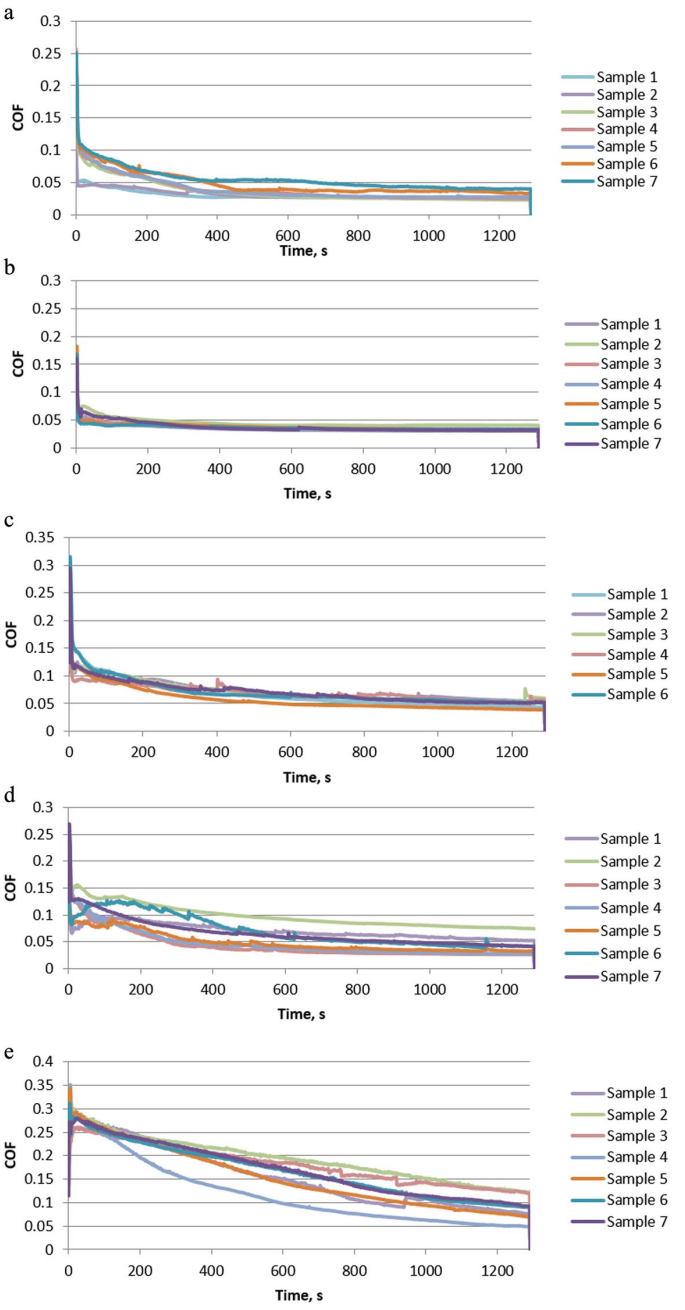


*Fig. 5. Maximum coefficient of friction versus time for sliding pairs with textured discs containing circular dimples of density: 5 (a), 9 (b), 14 (c), 17 (d) and 22% (e)*

was especially visible for textured sliding pairs. The scatter of friction force in the final test part was the lowest. The untextured assembly is characterized by high resistance to motion and the highest scatter of the coefficient of friction among all tested sliding pairs. The highest pit-area ratio of circular dimples also led to a high coefficient of friction (especially initial) with comparatively high scatters. The friction force was also high for the assembly containing oil pockets of sandglass shape with the lowest dimple density. The other sliding pairs were characterized by small average values and scatters of the coefficient of friction. Surface texturing caused a substantial reduction in the friction coefficient compared to the untextured assembly for circular dimples with densities of 5 and 9% and for oil pockets of sandglass shape with densities of 9, 17 and 22%. Among circular dimples, pit-area ratios of 5 and 9% led to similar coefficients of friction. However, the smallest scatter of friction coefficient was achieved for a dimples density of 9%. Further increase in the pit-area ratio caused an increase in the coefficient of friction, especially for the highest dimple density of 22%.

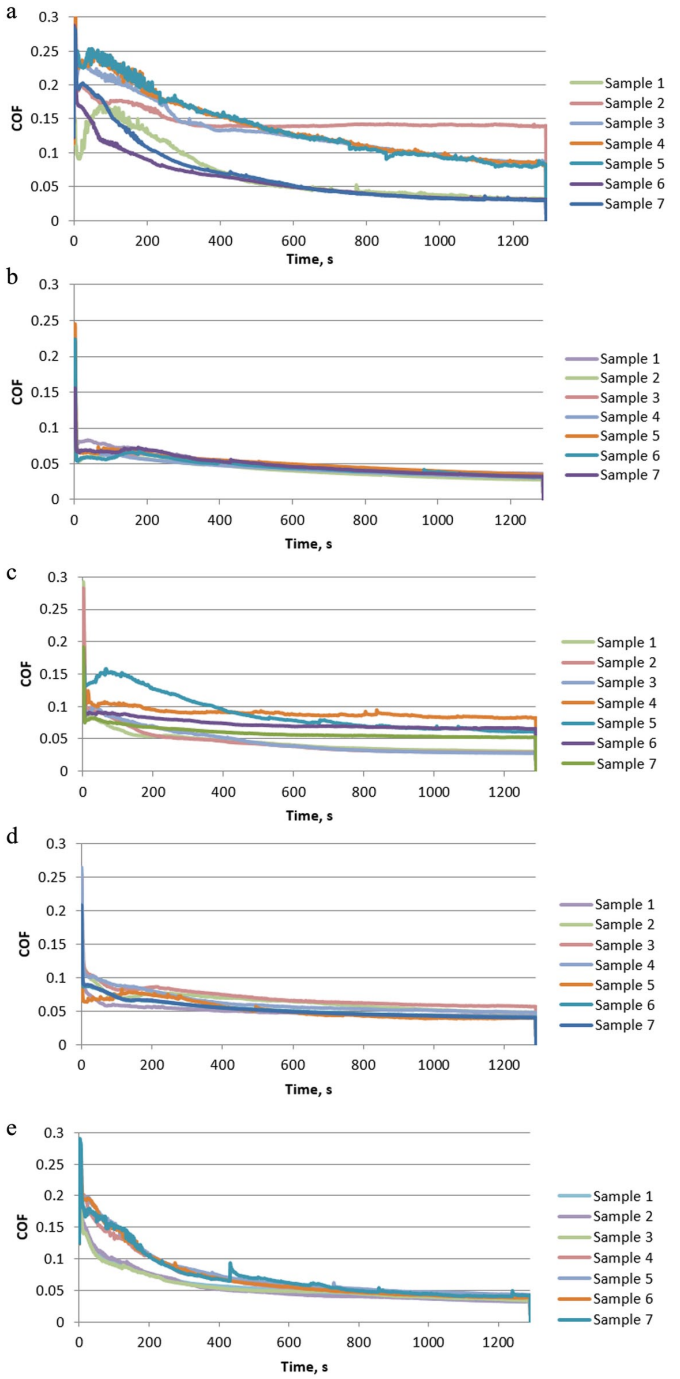


*Fig. 6. Maximum coefficient of friction versus time for sliding pairs with textured discs containing oil pockets of sandglass shape with density: 5 (a), 9 (b), 14 (c), 17 (d) and 22% (e)*

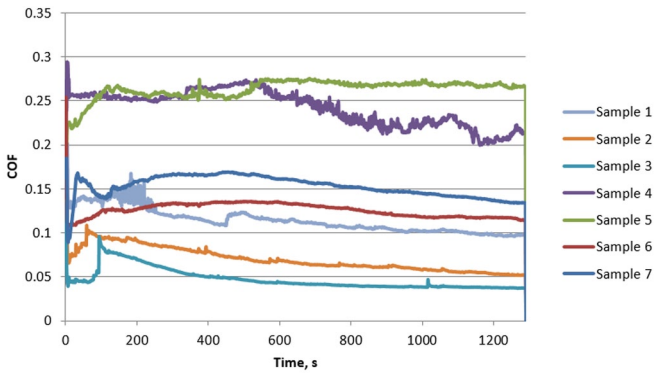


*Fig. 7. Maximum coefficient of friction versus time for an untextured sliding pair*

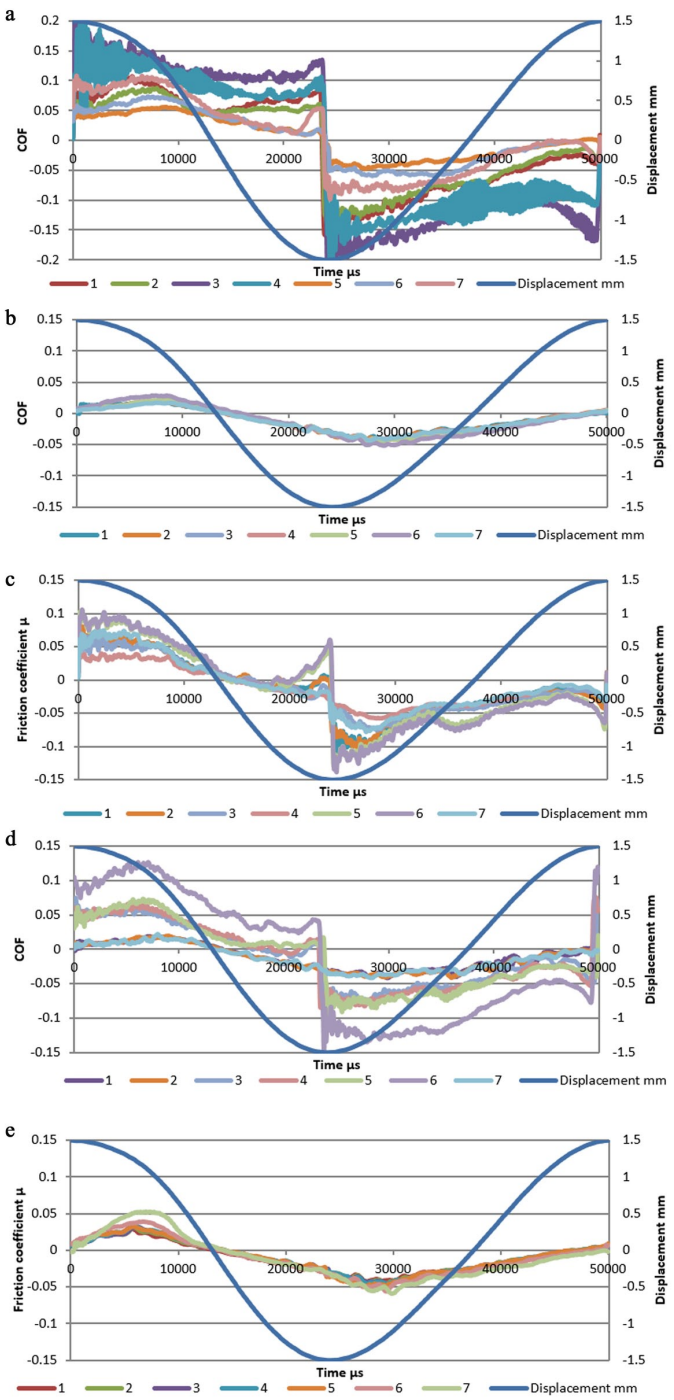


*Fig. 8. The coefficient of friction and displacement within one stroke for untextured assembly (a) and for sliding pairs containing circular dimples with pit-area ratio of 9% (b), circular dimples with pit-area ratio of 22% (c), oil pockets of sandglass shape with pit-area ratio of 5% (d) and oil pockets of sandglass shape with pit-area ratio of 17% (e)*

Among the oil pockets of the sandglass shape, the pit-area ratio of 9% led to the smallest average values and scatters of the coefficient of friction. Therefore, independently of oil pocket shape, the best tribological performance was achieved for the pit-area ratio of 9%.

Figure 8 presents the coefficient of friction and displacement versus time within one stroke (during 0.05 seconds) for selected sliding pairs after 20 minutes (high resolution analysis).

When the untextured assembly was tested (Figure 8a), the highest coefficients of friction were obtained in the reversal points. Similar graphs were obtained for sliding pairs containing textured discs characterized by comparatively high resistance to motion: containing circular dimples with a density of 22% (Figure 8c), oil pockets of

*Table 2 The average values and standard deviations of the coefficient of friction obtained in the initial ( 200-400 s), final (1100-1300 s) parts of the tests and in the entire tests (200-1300 s)*

| **Initial: 200-400 s** | | | | | | | | | | | |
|---|---|---|---|---|---|---|---|---|---|---|---|
| | **circle 5%** | **circle 9%** | **circle 14%** | **circle 17%** | **circle 22%** | **sandg-lass 5%** | **sandg-lass 9%** | **sandg-lass 14%** | **sandg-lass 17%** | **sandg-lass 22%** | **reference** |
| **Average** | 0.048 | 0.040 | 0.079 | 0.076 | 0.209 | 0.128 | 0.056 | 0.071 | 0.066 | 0.075 | 0.153 |
| **Standard deviation** | 0.015 | 0.003 | 0.008 | 0.023 | 0.023 | 0.04 | 0.005 | 0.021 | 0.009 | 0.013 | 0.072 |
| **Final: 1100-1300 s** | | | | | | | | | | | |
| | circle 5% | circle 9% | circle 14% | circle 17% | circle 22% | sandglass 5% | sandglass 9% | sandglass 14% | sandglass 17% | sandglass 22% | reference |
| **Average** | 0.031 | 0.033 | 0.052 | 0.042 | 0.095 | 0.070 | 0.032 | 0.049 | 0.045 | 0.038 | 0.131 |
| **Standard deviation** | 0.009 | 0.003 | 0.005 | 0.016 | 0.025 | 0.037 | 0.002 | 0.020 | 0.005 | 0.004 | 0.076 |
| **Mean: 200-1300 s** | | | | | | | | | | | |
| | **circle 5%** | **circle 9%** | **circle 14%** | **circle 17%** | **circle 22%** | **sandg-lass 5%** | **sandg-lass 9%** | **sandg-lass 14%** | **sandg-lass 17%** | **sandg-lass 22%** | **reference** |
| **Average** | 0.037 | 0.035 | 0.063 | 0.054 | 0.145 | 0.099 | 0.042 | 0.057 | 0.053 | 0.052 | 0.143 |
| **Standard deviation** | 0.013 | 0.003 | 0.011 | 0.022 | 0.048 | 0.044 | 0.008 | 0.021 | 0.01 | 0.014 | 0.077 |

sandglass shape with a density of 5% (Figure 8d) and 14%. When the friction coefficient was comparatively low, the maximum friction coefficient occurred after the reversal point, this behavior happened for assemblies with circular dimples of 5%, 9% (Figure 8b), and with oil pockets of sandglass shape with densities of 9%, 17% (Figure 8d) and 22%. When other assemblies were tested, for some repetitions, the maximum friction force was obtained at the reversal points (circular dimples of densities 14 and 17%), for other repetitions shifts of maximum friction coefficient appeared.

Figure 9 presents photos of the selected disc samples after tribological tests. The disc wear had an abrasive character. The wear levels were small. The wear tracks were visible mainly on the untextured sample, on the sample containing circular dimples of the highest pit-area ratio of 22%, and on the sample containing oil pockets of sandglass shape of the lowest density, of 5% – Figure 10.

In most cases, the surface texturing of the disc caused decreases in the average values and scatters of the coefficient of friction. Reductions were smaller in the final parts of the tests compared to the initial test portions. This tendency can be explained by the shapes of the friction force versus time. For textured assemblies, after initial fluctuations, the coefficient of friction decreased with time. Friction reduction occurred in the initial test parts, up to 70 seconds. This reduction is the result of better matching of co-acting pairs as the test

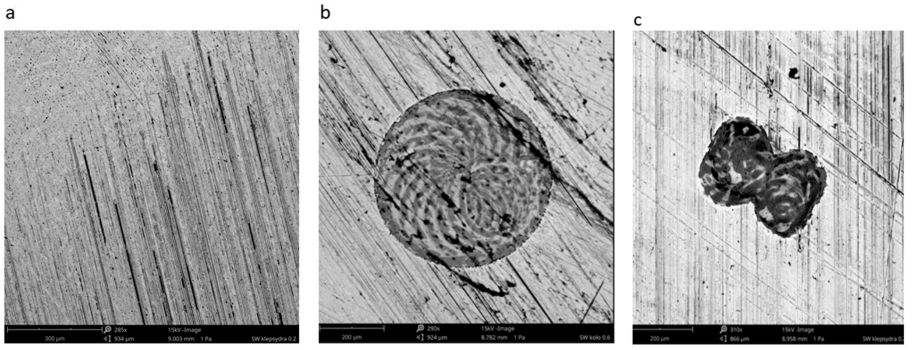


*Fig. 10. SEM views of (a) untextured disc and of the textured disc with spherical dimple of the pit-area ratio of 22% (b), and of the textured disc with oil pocket of sandglass shape of pit-area ratio of 5% (c) after tribological tests*

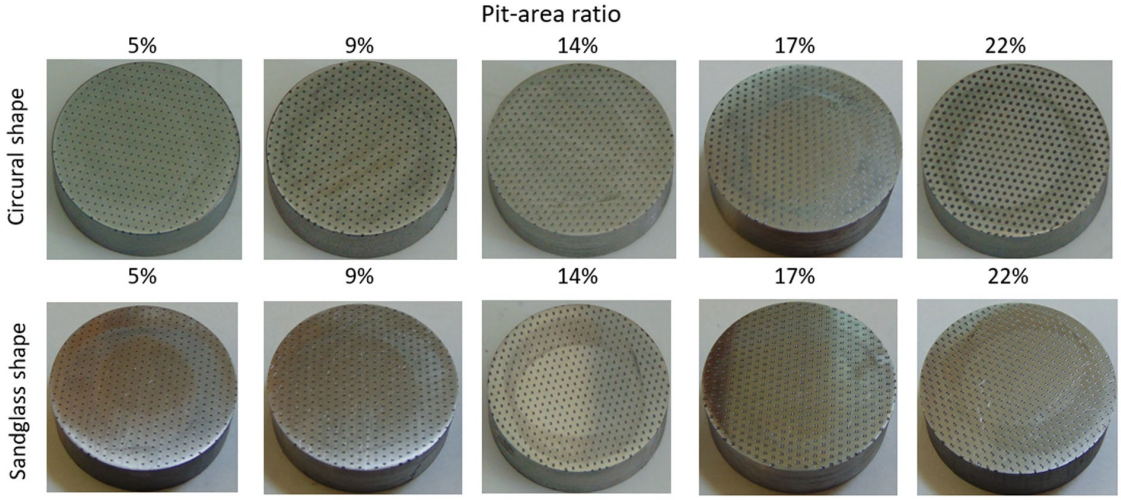


*Fig. 9. Photos of textured disc surfaces after the tests*

progressed. The presence of dimples also helped create hydrodynamic lift, decreasing the friction coefficient. The highest reduction in the average coefficient of friction was about 4.5 times.

Untextured sliding pairs showed different behaviors. In five cases, the coefficient of friction obtained the highest value after about 500 seconds and then decreased; the final coefficients of friction were higher than those obtained for most of the textured sliding pairs. In two cases, the maximum value of the friction coefficient was obtained after about 100 seconds, and then the friction coefficient decreased with time; in these cases, the final coefficients of friction were similar to those obtained for textured assemblies. Due to the lack of dimples, in most cases it was difficult to match sliding surfaces, therefore the coefficient of friction increased slowly. When the surfaces were correctly matched, the coefficient of friction decreased. In other cases, the surface matching appeared faster. Different shapes of the friction coefficient curves and high scatters of the coefficient of friction were caused by non-uniformity of the untextured (lapped) disc.

The analysis of the friction coefficient within one stroke is interesting (Figure 8). For untextured sliding assemblies due to small oil film thickness the highest friction force occurred at the reversal points. Disc surface texturing led to not only a decrease in the coefficient of friction but also to a shift of the maximum friction coefficient. The last behavior has not been observed in other experiments [15, 17, 27, 28, 34], under reciprocating motion, but it was found only in [1]. This shift was observed for assemblies characterized by the smallest values of the friction coefficient. This performance resulted probably from oil pockets presence, which caused an increase of oil film thickness at the reversal points. Inertia of oil caused the shift of the maximum values of the friction force. Lu et al. [17] observed directional friction effect for sloped bottoms of dimples in line contact. However, this effect was not detected in the present study.

Although surface texturing in most cases led to reductions in values and scatter of the friction forces, the worst situation occurred for circular dimples of the highest pit-area ratio and for oil pockets of sandglass shape with the smallest density.

The high friction value and variation of assembly with dimples of sandglass shape with pit-area ratio of 5% were probably caused by the smallest width of oil pockets perpendicular to the sliding direction. This width of oil pockets of sandglass shape was about 0.6 of the diameter of spherical dimples. For the smallest pit-area ratio of 5%, there was probably too low length of contact between the oil pockets and the counter-sample perpendicular to the sliding direction, which caused behavior similar to the untextured sliding assembly. On the other hand, the spherical dimples of 5% density, because of their higher widths orthogonally to the sliding direction, caused high reductions in values and scatters in the coefficient of friction. For the highest pit-area ratio of 22%, the lengths of spherical dimples on sliding direction were probably too high, for comparatively low sliding speed, resulting in large values and scatters of the coefficient of friction. Yu et al. [33] obtained also high friction for circular dimples of large density for comparatively small normal load.

The spherical dimples had a similar depth, except for those with the smallest pit-area ratio of 5% (of the highest depth). Similarly, textured discs with oil pockets of sandglass shape were characterized by similar depth, except for those of the highest density (of the smallest depth). From the results of research, it seems that dimple depth did not affect tribological performance of sliding pairs. In most cases, the bottoms of the oil pockets were not flat. However, the effect of rough bottom on tribological performance appears to be small. This finding was in accordance with that obtained by Qiu and Raeymaekers [22]. They found that the effect of random Gaussian roughness inside dimples on the load carrying capacity of the parallel sliding bearing was negligible.

## 4. Conclusions

1. Laser texturing of the disc surfaces in most cases led to reductions in friction force values and fluctuations in reciprocating motion. The decrease in the friction coefficients was up to 4.5 times. The beneficial effects of laser texturing were achieved for both oil pockets of spherical and sandglass shapes.
2. Laser texturing caused a substantial reduction in the friction coefficient compared to the untextured assembly for circular oil pockets with pit-area ratios of 5 and 9% and for oil pockets of sandglass shape with pit-area ratios of 9, 17, and 22%. Independently of the shape of the oil pocket shapes, the best tribological behavior was achieved for the pit-area ratio of 9%.
3. For textured sliding assemblies, the highest coefficient of friction was obtained for circular dimples of the highest density of 22% and for oil pockets of sandglass shape of the smallest density of 5%.
4. Disc surface texturing caused the shift of the maximum friction coefficient from the transversal points within one stroke. This shift was observed for assemblies characterized by low values of the friction coefficient.
5. Were levels of discs were small. Tracks of wear were visible mainly on untextured discs and on disc samples corresponding to the high coefficients of friction.

***Acknowledgments***

*This work was supported by the National Science Center (Decision No. 2018/31/B/ST8/02946) "The effect of disc surface texturing on the tribological properties of pin-on-disc assembly".*

## References

1. Akbarzadeh A, Khonsari M M. Effect of untampered plasma coating and surface texturing on friction and running-in behavior of piston rings. Coatings 2018; 8: 110, https://doi.org/10.3390/coatings8030110.
2. Atulkar A, Pandey R K, Subbarao P M V. Role of textured piston rings/liners in improving the performance behaviours of IC engines: A review with vital findings. Surface Topography: Metrology and Properties 2021; 9: 023002, https://doi.org/10.1088/2051-672X/ac0a36.
3. Costa H L, Hutchings I M. Hydrodynamic lubrication of textured steel surfaces under reciprocating sliding conditions. Tribology International 2007; 40(8): 1227 1238, https://doi.org/10.1016/j.triboint.2007.01.01.
4. Etsion I. State of the art in laser surface texturing. ASME Journal of Tribology 2005; 125: 248–253, https://doi.org/10.1115/1.1828070.
5. Gachot C, Rosenkranz A, Hsu S M, Costa H L. A critical assessment of surface texturing for friction and wear improvement. Wear 2017; 372-373: 21-41, https://doi.org/10.1016/j.wear.2016.11.020.
6. Galda L, Dzierwa A, Sep J, Pawlus P. The effect of oil pockets shape and distribution on seizure resistance in lubricated sliding. Tribology Letters 2010; 37: 301–311, https://doi.org/10.1007/s11249-009-9522-7.
7. Grabon W, Koszela W, Pawlus P, Ochwat S. Improving tribological behaviour of piston ring-cylinder liner frictional pair by liner surface texturing. Tribology International 2013; 61: 102–108, https://doi.org/10.1016/j.triboint.2012.11.027.
8. Grabon W, Pawlus P, Sep J. Tribological characteristics of one-process and two-process cylinder liner honed surfaces under reciprocating sliding conditions. Tribology International 2010; 43: 1882-1892, https://doi.org/10.1016/j.triboint.2010.02.003.
9. Grabon W, Pawlus P, Wos S, Koszela W, Wieczorowski M. Evolutions of cylinder liner surface texture and tribological performance of piston ring-liner assembly. Tribology International 2018; 127: 545-556, https://doi.org/10.1016/j.triboint.2018.07.011.

10. Holmberg K, Andersson P, Erdemir A. Global energy consumption due to friction in passenger cars. Tribology International 2012; 47: 221-234, https://doi.org/10.1016/j.triboint.2011.11.022.
11. Hua X, Sun J, Zhang P, Ge H, Yonghong F, Jinghu J, Yin B. Research on discriminating partition laser surface micro-texturing technology of engine cylinder. Tribology International 2016; 98: 190–196, https://doi.org/10.1016/j.triboint.2016.02.010.
12. Kang Z, Fu Y, Zhou D, Wu Q, Chen T, He Y, Su X. Reducing engine oil and fuel consumptions by multidimensional laser surface texturing on cylinder surface. Journal of Manufacturing Processes 2021; 64: 684–693, https://doi:10.1016/j.jmapro.2021.01.052.
13. Koszela W, Pawlus P, Reizer R, Liskiewicz T. The combined effect of surface texturing and DLC coating on the functional properties of internal combustion engines. Tribology International 2018; 127: 470-477, https://doi.org/10.1016/j.triboint.2018.06.034.
14. Kresak J, Peterka P, Ambrisko L, Mantič M. Friction lining coefficient of the drive friction pulley. Eksploatacja i Niezawodnosc – Maintenance and Reliability 2021; 23(2): 338-345, http://doi.org/10.17531/ein.2021.2.13.
15. Lu P, Wood R J K, Gee M G, Wang L, Pfleging W. A novel surface texture shape for directional friction control. Tribology Letters 2018: 66: 51, https://doi.org/10.1007/s11249-018-0995-0.
16. Lu P, Wood R J K, Gee M G, Wang L, Pfleging W. The friction reducing effect of square-shaped surface textures under lubricated line-contacts - An experimental study. Lubricants 2016; 4(3): 26, https://doi.org/10.3390/lubricants4030026.
17. Lu P, Wood R J K, Gee M G, Wang L, Pfleging W. The use of anisotropic texturing for control of directional friction. Tribology International 2017; 113: 169–181, https://doi.org/10.1016/j.triboint.2017.02.005.
18. Morris N, Leighton M, De la Cruz M, Rahmani R, Rahnejat H, Howell-Smith S. Combined numerical and experimental investigation of the micro-hydrodynamics of chevron-based textured patterns influencing conjunctional friction of sliding contacts. Proceedings of the Institution of Mechanical Engineers, Part J: Journal of Engineering Tribology 2015;. 229(4): 316–335, https://doi.org/10.1177/1350650114559996.
19. Morris N, Rahmani R, Rahnejat H, King P D, Howell-Smith S. A numerical model to study the role of surface textures at top dead center reversal in the piston ring to cylinder liner contact. Journal of Tribology 2016; 138(2): 021703, https://doi.org/10.1115/1.4031780.
20. Nilsson B, Rosen B G, Thomas T R, Wiklund D. Oil pockets and surface topography: mechanism of friction reduction, in: Proceedings of the XI International Colloquium on Surfaces, Chemnitz, Germany, 2004.
21. Pawlus P. A study on the functional properties of honed cylinder surface during running-in. Wear 1994; 176: 247-254, https://doi.org/10.1016/0043-1648(94)90153-8.
22. Qiu M, Raeymaekers B. The load-carrying capacity and friction coefficient of incompressible textured parallel slider bearings with surface roughness inside the texture features. Proceedings of the Institution of Mechanical Engineers, Part J: Journal of Engineering Tribology 2014; 229(4): 547–556, https://doi.org/10.1177/1350650114545352.
23. Rosenkranz A, Grützmacher P, Gachot C, Costa H. Surface texturing in machine elements - A critical discussion for rolling and sliding contacts. Advanced Engineering Materials 2019; 21(8): 1900194, https://doi.org/10.1002/adem.201900194.
24. Samtochi M, Vignale M, Giusti F. A study on the functional properties of the honed surface. CIRP Annals 1982; 31: 432-434, https://doi.org/10.1016/S0007-8506(07)63342-3.
25. Sawczuk W. Analytical model coefficient of friction (COF) of rail disc brake on the basis of multi-phase stationary tests. Eksploatacja i Niezawodnosc – Maintenance and Reliability 2018; 20(1): 57-67, http://dx.doi.org/10.17531/ein.2018.1.8.
26. Shen C, Khonsari M M. Numerical optimization of texture shape for parallel surfaces under unidirectional and bidirectional sliding. Tribology International 2015; 82: 1–11, https://doi.org/10.1016/j.triboint.2014.09.022.
27. Vladescu S C, Ciniero A, Tufail K, Gangopadhyay A, Reddyhoff T. Looking into a laser textured piston ring-liner contact. Tribology International 2017; 115: 140–153, https://doi:10.1016/j.triboint.2017.04.051.
28. Vladescu S C, Olver A V, Pegg G, Reddyhoff T. The effects of surface texture in reciprocating contacts - an experimental study. Tribology International 2015; 82: 28–42, https://doi.org/10.1016/j.triboint.2014.09.015.
29. Wang W, Huang Z, Shen D, Kong L, Li S. The effect of triangle-shaped surface textures on the performance of the lubricated point-contacts. Journal of Tribology 2013; 135(2): 021503, https://doi.org/10.1115/1.4023206.
30. Wos S, Koszela W, Pawlus P. Comparing tribological effects of various chevron-based surface textures under lubricated unidirectional sliding. Tribology International 2020; 146: 106205, doi:10.1016/j.triboint.2020.10620.
31. Yin B, Xu B, Jia H, Zhou H, Fu Y, Hua X. Effects of the array modes of laser-textured micro-dimples on the tribological performance of cylinder liner–piston ring. Proceedings of the Institution of Mechanical Engineers, Part J: Journal of Engineering Tribology 2018; 232: 871-881, https://doi.org/10.1177/1350650117732718.
32. Yin B, Zhou H, Xu B, Jia H. The influence of roughness distribution characteristic on the lubrication performance of textured cylinder liners. Industrial Lubrication and Tribology 2019; 71(3), 486-493, https://doi.org/10.1108/ilt-07-2018-0258.
33. Yu H, Deng H, Huang W, Wang X. The effect of dimple shapes on friction of parallel surfaces. Proceedings of the Institution of Mechanical Engineers, Part J: Journal of Engineering Tribology 2011; 225(8): 693–703, https://doi.org/10.1177/1350650111406045.
34. Yuan S, Huang W, Wang X. Orientation effects of micro-grooves on sliding surfaces. Tribology International 2011; 44: 1047-1054, https://doi.org/10.1016/j.triboint.2011.04.007.
35. Zhang H, Hua M, Dong G N, Zhang D Y, Chin K S. A mixed lubrication model for studying tribological behaviors of surface texturing. Tribology International 2016; 93: 583–592, https://doi.org/10.1016/j.triboint.2015.03.027.
36. Zhang Y L, Zhang X G, Matsoukas G. Numerical study of surface texturing for improving tribological properties of ultra-high molecular weight polyethylene. Biosurface and Biotribology 2015; 1(4): 270–277, https://doi.org/10.1016/j.bsbt.2015.11.003.